NOTES AND CORRESPONDENCE

Parameterizations for the Absorption of Solar Radiation by Water Vapor and Ozone

MING-DAH CHOU

Laboratory for Atmospheres, NASA/Goddard Space Flight Center, Greenbelt, Maryland

KYU-TAE LEE

Department of Atmospheric Science, Kangnung National University, Kangnung, South Korea

25 May 1995 and 14 November 1995

1. Introduction

In parameterizing the solar heating due to water vapor and ozone, it is highly desirable that the transmission function is given by Beer's law (i.e., equivalent to monochromatic transmission) so that multiple-scattering radiative transfer schemes can be applied. Water vapor absorbs solar radiation in the wavelengths > 0.5 μm. Chou (1992) developed an efficient parameterization using the k-distribution method for the water vapor transmission function in the near infrared (IR) (0.7–3.85 μm). In the thermal spectral region ($\lambda > 3.85$ μm), the solar flux is small and was not included in the parameterization. However, it was found by Kratz and Cess (1985) and Ramaswamy and Freidenreich (1991) that atmospheric solar heating in this spectral region was small but not negligible. Therefore, we extend the parameterization of Chou (1992) from the near IR to the thermal IR (10 μm). Between 0.5 and 0.7 μm, there are four weak visible absorption bands. Line-by-line calculations show that for a clear atmosphere and a solar zenith angle of 60°, the absorption of solar radiation by water vapor is only 2 W m^{-2}. Therefore, we also neglect the absorption due to water vapor in this spectral region. In addition to extending the spectral range to the thermal IR, we investigate in this note the characteristics of vertical heating profile when the k-distribution method is used to compute the transmission function. This note uses the 1992 version of the molecular line parameters compiled at Air Force Geophysical Laboratory (Rothman et al. 1987) instead of the 1986 version as used by Chou (1992).

Ozone absorbs solar radiation in the UV and visible wavelengths, $\lambda < 0.7$ μm. In the PAR (photosynthetically active radiation) band (0.4 μm $< \lambda <$ 0.7 μm), solar radiation reaching the surface is critical in the biosphere–atmosphere interaction. In the UV-A band (0.32 μm $< \lambda <$ 0.40 μm), the atmosphere is nearly transparent, and solar radiation can freely penetrate to the surface. In the UV-B (0.28 μm $< \lambda <$ 0.32 μm) and UV-C (0.10 μm $< \lambda <$ 0.28 μm) bands, most of the solar radiation is absorbed in the middle atmosphere, which provides energy for photochemical reactions.

The ozone absorption coefficient varies by several orders of magnitude, but smoothly, with wavelengths. In order to enhance the speed of computation, Chou (1992) parameterized the absorption of UV and visible radiation by grouping the spectrum into four bands with boundaries different from the four bands cited above. The PAR and UV-A bands were combined, and the fluxes in these two bands could not be separately computed. Sections of UV-B and UV-C bands were also combined. This spectral grouping imposes difficulties in the studies of photochemical processes in the middle atmosphere and the biosphere–atmosphere interactions at the surface. To avoid these difficulties, we divide the UV and visible spectrum into eight bands so that solar fluxes in the PAR, UV-A, UV-B, and UV-C can be separately computed.

The absorption of solar radiation by oxygen and CO_2 can be computed using the method given by Chou (1990), which is independent of the parameterizations addressed in this note.

2. Absorption due to water vapor

The transmission between the top of the atmosphere and the pressure level p is given by

$$\tau_\nu(p) = e^{-1/(g\mu_0)\int_0^p k_\nu(p'T')q(p')dp'}, \qquad (1)$$

where ν is the wavenumber, μ_0 is the cosine of the solar zenith angle, k is the absorption coefficient, T is the temperature, q is the specific humidity, and g is the gravitational acceleration.

Corresponding author address: Dr. Ming-Dah Chou, Laboratory for Atmospheres, Climate and Radiation Branch, NASA/GSFC, Code 913, Greenbelt, MD 20771.

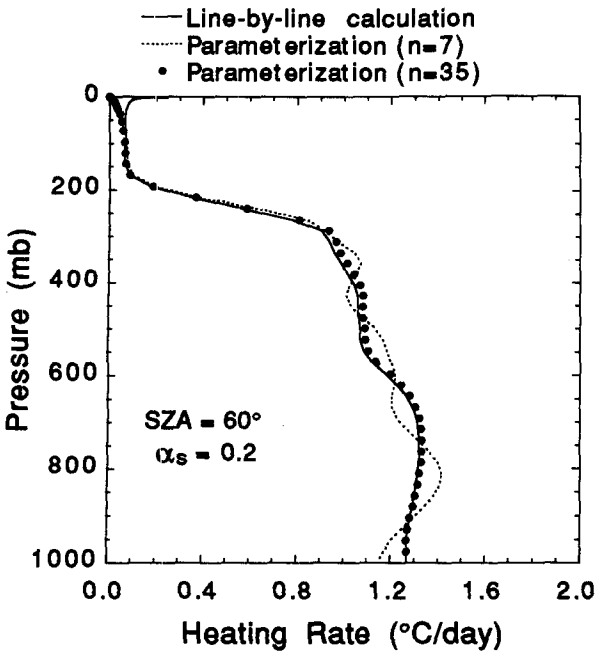

FIG. 1. Heating profiles due to the absorption of solar radiation by water vapor computed for a midlatitude summer atmosphere. SZA and α_s are the solar zenith angle and the surface albedo, respectively.

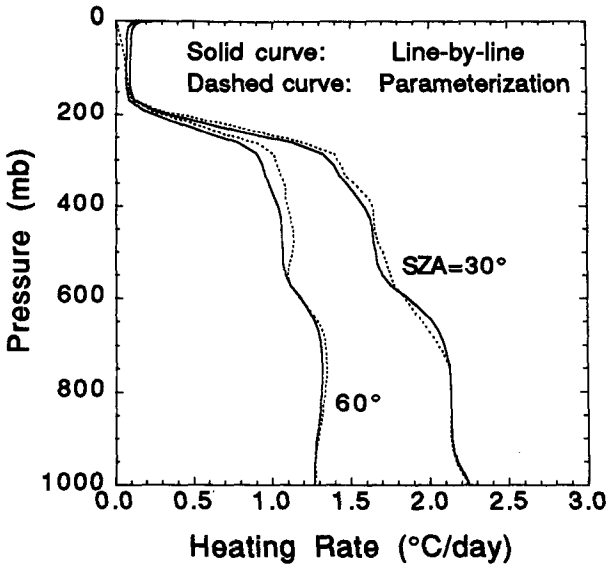

FIG. 3. Heating profiles due to the absorption of solar radiation by water vapor in a midlatitude summer atmosphere. The dashed curves are computed using the k-distribution method with ten k-intervals given in Table 1.

The variation of k with ν depends strongly on pressure but only weakly on temperature. Near the center of a molecular line, absorption is strong and quickly saturated (i.e., complete absorption) within a relatively short distance. Therefore, accurate calculations of the absorption coefficient near line centers are not as important as in the region away from the centers where the absorption coefficient increases with pressure. Chou and Arking (1981) used a simple yet efficient way of taking into account the effect of pressure and temperature on absorption, which scaled the absorption coefficient according to

$$k_\nu(p, T) = k_\nu(p_r, T_r)\left(\frac{p}{p_r}\right)^m h(T, T_r), \qquad (2)$$

where m is an empirical constant slightly less than 1, p_r and T_r are the reference pressure and temperature, respectively, and h is a simple scaling function of temperature. For reasons explained by Chou and Arking (1981), the reference pressure is chosen to be 300 mb to achieve a maximum accuracy in transmittance calculations. With p_r = 300 mb, m is empirically determined to be 0.8. It is found that solar heating calculations are not sensitive to m for $0.7 < m < 0.9$. A temperature of 240 K is chosen for the reference temperature.

When the scaling approximation of (2) is used, the mean transmission function of a narrow spectral interval $\Delta\nu_i$, where the extraterrestrial solar flux can be considered as constant, can be written as

$$\tau_i(p) = \frac{1}{\Delta\nu_i}\int_{\Delta\nu_i} e^{-k_\nu(p_r,T_r)w(p)/\mu_0} d\nu, \qquad (3)$$

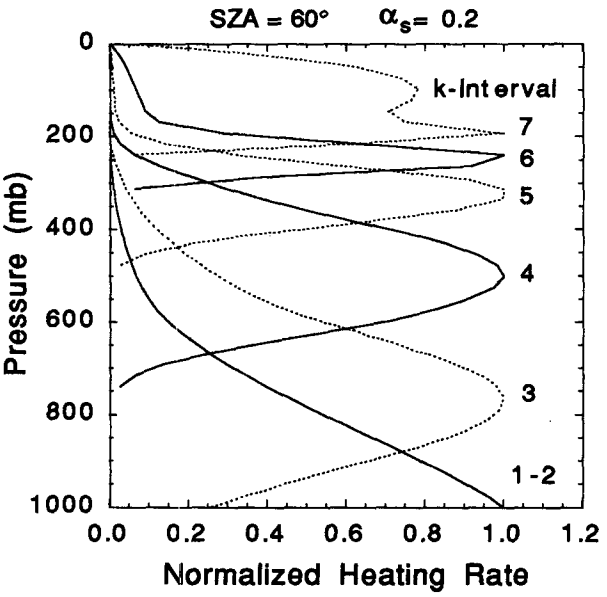

FIG. 2. The normalized water vapor heating profiles attributable to seven individual terms of the k-distribution function ($\Delta \log_{10} k = 1.0$). These profiles are computed for a midlatitude summer atmosphere.

TABLE 1. The flux-weighted k-distribution function, Δg, in the near and thermal infrared region for $p_r = 300$ mb and $T_r = 240$ K. The parameter k is the absorption coefficient (g^{-1} cm^2).

Interval	k	Δg (0.7–10 μm)	Δg (0.7–1.22 μm)	Δg (1.22–2.27 μm)	Δg (2.27–10.0 μm)
1	0.0010	0.29983	0.20673	0.08236	0.01074
2	0.0133	0.05014	0.03497	0.01157	0.00360
3	0.0422	0.04555	0.03011	0.01133	0.00411
4	0.1334	0.03824	0.02260	0.01143	0.00421
5	0.4217	0.02965	0.01336	0.01240	0.00389
6	1.334	0.02280	0.00696	0.01258	0.00326
7	5.623	0.02321	0.00441	0.01381	0.00499
8	31.62	0.01230	0.00115	0.00650	0.00465
9	177.8	0.00515	0.00026	0.00244	0.00245
10	1000.0	0.00239	0.00000	0.00094	0.00145

where the scaled water vapor amount w is given by

$$w(p) = \int_0^p \left(\frac{p'}{p_r}\right)^m h(T', T_r) q(p') \frac{dp'}{g}. \quad (4)$$

As can be seen in (3), transmittances at wavenumbers with the same value of $k(p_r, T_r)$ are all identical irrespective of atmospheric conditions. The integration over wavenumbers can then be replaced by the integration over k-intervals using the k-distribution method,

$$\tau_i(p) = \sum_{j=1}^{n} f_i(k_j) e^{-k_j w(p)/\mu_0}, \quad (5)$$

where n is the number of k-intervals, $f_i(k)$ is the k-distribution function in the spectral interval i for $p_r = 300$ mb, and $T_r = 240$ K.

Solar fluxes over the near and thermal IR spectral range (0.7–10 μm) are computed from

$$F(p) = \mu_0 \sum_i (S_i \Delta\nu_i) \tau_i(w(p), \mu_0),$$

$$= S_0 \mu_0 \sum_{j=1}^{n} e^{-k_j w(p)/\mu_0} \Delta g_j, \quad (6)$$

TABLE 2. Net solar fluxes (downward minus upward) at the top of the atmosphere and at the surface for a midlatitude summer atmosphere. The surface albedo is set to 0.2. Term θ_0 is the solar zenith angle. The units of fluxes are watts per squared meter.

	Top		Surface	
	$\theta_0 = 30°$	$\theta_0 = 60°$	$\theta_0 = 30°$	$\theta_0 = 60°$
	Water vapor (0.7–10.0 μm)			
Line-by-line calculation	543.4	315.0	369.4	202.3
Parameterization	544.0	315.4	368.2	201.5
	Ozone + Rayleigh scattering (0.175–0.7 μm)			
High-resolution calculation	429.0	236.2	394.5	211.4
Parameterization	429.0	235.9	394.3	211.0

where S_0 is the total extraterrestrial solar flux, $S_i \Delta\nu_i$ is the extraterrestrial solar flux in the spectral interval i, and Δg_j is the flux-weighted k-distribution function given by

$$\Delta g_j = \sum_i (S_i \Delta\nu_i) f_i(k_j)/S_0. \quad (7)$$

The k-distribution function, $f_i(k)$, is derived from the line by line method (cf. Chou 1992) for narrow spectral intervals with $\Delta\nu = 40$ cm^{-1}. The function Δg_j is independent of atmospheric conditions and is accurately precomputed.

Finally, the heating rate of a layer with a thickness Δp is computed from

$$\frac{\partial T}{\partial t} = -\frac{g}{c_p} \frac{(F(p + \Delta p) - F(p))}{\Delta p}, \quad (8)$$

where c_p is the specific heat of air at constant pressure.

With Δg precomputed, fluxes and heating rate can be easily derived from (6) and (8). Figure 1 shows the heating profiles due to water vapor for a typical midlatitude summer atmosphere (McClatchey et al. 1972), a solar zenith angle of 60°, and a surface albedo of 0.2. Note that calculations of the upward flux reflected by the surface is similar to that of (6), except the water vapor amount between the level p and the surface is scaled by 1.66 instead of μ_0^{-1}. The solid curve is computed using the line-by-line method with a spectral resolution of 0.01 cm^{-1}. The dashed curve and dots are derived using the k-distribution method of (6) with $n = 7$ and 35, respectively. For the case of $n = 35$, the parameterization agrees very well with the line by line calculations. When n decreases to 7 ($\Delta \log_{10} k = 1.0$), the heating profile shows a large oscillation. Because of the pressure-scaling in (2), the heating in the stratosphere is underestimated.

To investigate the cause of the oscillation, contributions from each of the 7 k-intervals to the total heating are computed. From (6) and (8), the heating due to the jth k-interval is given by

$$\Gamma_j(p) = C_j e^{-k_j w(p)/\mu_0} \frac{dw}{dp}, \quad (9)$$

where C_j ($=S_0 k_j \Delta g_j$) is a constant for a given k. This partial heating is a product of two functions; one decreases rapidly with increasing pressure and the other increases rapidly with increasing pressure. Therefore, it has a distinct peak at a height increasing with the magnitude of k. Figure 2 shows the partial heating profiles (with maxima normalized to 1) of the individual k-intervals. The first two intervals are for small values of k and have a peak at the surface. In the lower and middle troposphere, the peaks of the normalized partial heating profiles are widely separated, causing the total heating profile to oscillate.

When n increases to ten, the spacing between the peaks of the partial heating profiles decreases (not shown in the figures). Consequently, oscillation of the total heating profile is much reduced (Fig. 3). Table 1 lists values of k for the ten k-intervals and Δg for the 0.7–10-μm region and three subbands. The fluxes at the top of the atmosphere and at the surface given in Table 2 show that not only the heating rate but also the fluxes can be computed accurately with $n = 10$. By including the solar radiation in the spectral region 3.85–10 μm, the solar heating for a solar zenith angle of 60° increases by 2.7 W m^{-2} at the surface and by 5.8 W m^{-2} in the earth–atmosphere system (not shown in the table). Atmospheric heating increases slightly with a maximum of 0.06°C day^{-1} in the upper troposphere.

3. Absorption due to ozone

Ozone absorbs solar radiation in the wavelengths $\lambda < 0.7$ μm. The spectrum is divided into eight bands with ranges given in Table 3. In the UV-B and UV-C spectral regions, the absorption coefficient in each region is large and varies by two orders of magnitude. Therefore, each spectral region is divided into three bands. In the UV-A and PAR spectral regions, the absorption due to ozone is weak, and each spectral region is treated as one band. Following Chou (1992), the transmission function averaged over a band is first computed from

$$\tau'(u/\mu_0) = \frac{1}{S}\int_{\Delta\nu} S_\nu e^{-k_\nu u/\mu_0} d\nu, \tag{10}$$

where

$$S = \int_{\Delta\nu} S_\nu d\nu, \tag{11}$$

u is the ozone amount, and k_ν is the ozone absorption coefficient taken from WMO (1985). It is noted that k_ν is independent of pressure, and its dependence on temperature is negligible. An effective absorption coefficient, k_{eff}, for each of the eight bands is then derived from the following fitting,

$$e^{-k_{\text{eff}} u/\mu_0} = \tau'(u/\mu_0). \tag{12}$$

It is necessary to include the Rayleigh scattering in the calculation of solar heating due to ozone. Using the same procedures, an effective extinction coefficient due to Rayleigh scattering is also computed for each of the eight bands. The effective ozone absorption coefficient, the effective Rayleigh scattering coefficient, as well as the fractional extraterrestrial solar flux (S/S_0), are given in Table 3 for the eight bands.

The results for the transmission parameterization are shown in Fig. 4. The solid curves are computed using (10) with a spectral resolution of 0.001 μm (solid curves), and the dots are computed using the transmission parameterization,

$$\tau(u/\mu_0) = e^{-k_{\text{eff}} u/\mu_0}. \tag{13}$$

The maximum error in the transmittance is ≈0.05.

Figure 5 shows the heating profiles for the midlatitude summer atmosphere for three solar zenith angles,

TABLE 3. The spectral range, fractional solar flux, effective ozone absorption coefficient, and Rayleigh scattering optical thickness for the eight bands in the UV and visible spectral regions.

	Band	Spectral range (μm)	S/S_0	Ozone absorption coefficient (cm − atm)$^{-1}_{\text{stp}}$	Rayleigh scattering optical thickness (mb^{-1})
UV-C					
	1	0.175–0.225	0.00057	30.47	0.00604
	2	0.225–0.245 0.260–0.280	0.00367	187.24	0.00170
	3	0.245–0.260	0.00083	301.92	0.00222
UV-B					
	4	0.280–0.295	0.00417	42.83	0.00132
	5	0.295–0.310	0.00600	7.09	0.00107
	6	0.310–0.320	0.00556	1.25	0.00091
UV-A					
	7	0.320–0.400	0.05913	0.0345	0.00055
PAR					
	8	0.400–0.700	0.39081	0.0539	0.00012

30°, 60°, and 75°. The maximum heating rate error is $\approx 1°C\ day^{-1}$, which is considered small when compared with a maximum heating of $>20°C\ day^{-1}$. The downward fluxes at the top of the atmosphere and at the surface are given in Table 2. It can be seen in the table that flux errors induced by the parameterization are negligible.

Lacis and Hansen (1974) developed a broadband transmittance model for ozone absorption, while Briegleb (1992) presented a parameterization by dividing the UV and visible spectrum into eight bands as in this study. The ozone heating rates computed from these two methods are within $0.6°C\ day^{-1}$ of that shown in Fig. 5 (dashed curve) for a solar zenith angle of 60°. The solar radiation absorbed in the atmosphere by ozone alone, with a zero surface albedo and a solar zenith angle of 60°, as computed using the methods of Briegleb (1992), Lacis and Hansen (1974), and this study, are very close. They are 20.7, 22.0, and 22.3 $W\ m^{-2}$, respectively. Because Lacis and Hansen (1974) used a broadband transmittance model, it is difficult to explicitly compute the interaction between absorption due to ozone and scattering due to clouds, aerosols, and atmospheric molecules (i.e., Rayleigh scattering). On the other hand, the division of the eight spectral bands in Briegleb (1992) does not coincide with the ranges of PAR and UV-A, UV-B, and UV-C, as does in this study.

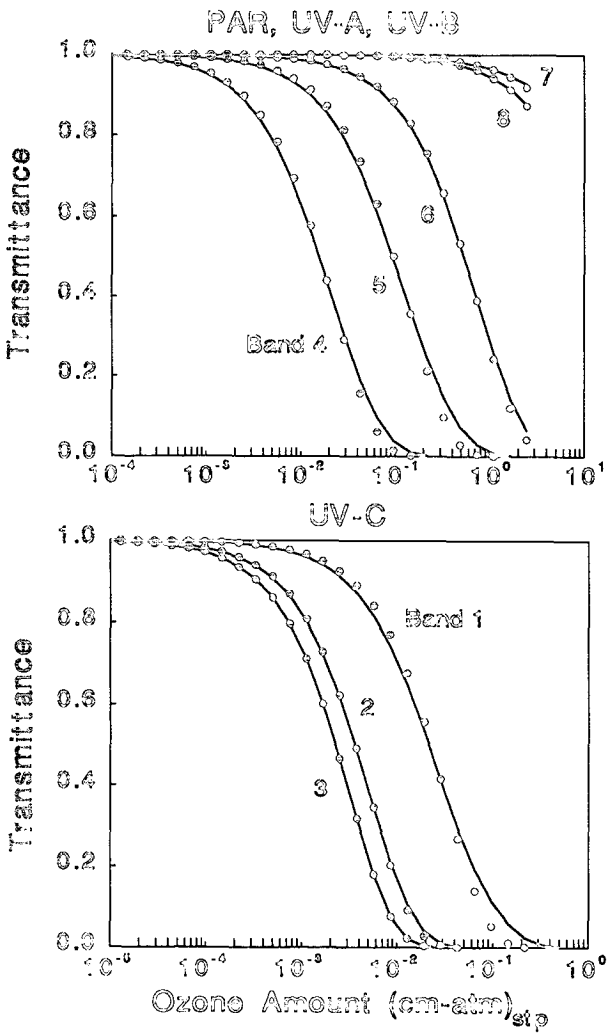

FIG. 4. The ozone transmission function for the eight bands in the UV and visible spectral regions. Solid curves are derived from high spectral resolution calculations, and the dots are derived from the parameterization.

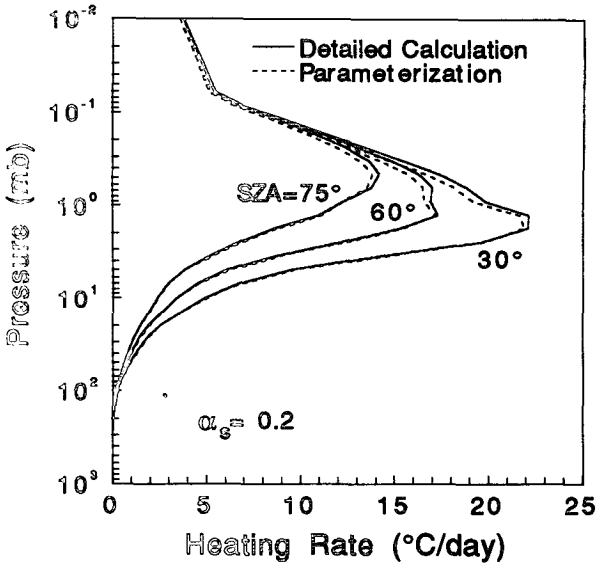

FIG. 5. Solar heating profiles in the UV and visible spectral regions for a midlatitude summer atmosphere. Ozone absorption and Rayleigh scattering are included in the calculations. SZA and α_s are the solar zenith angle and the surface albedo, respectively.

4. Concluding remarks

Efficient parameterizations for the absorption of solar radiation by water vapor and ozone are presented. The *k*-distribution method with simple pressure scaling is used in the calculations of solar heating due to water vapor. It is found that the contribution of each *k*-interval to the total heating has a distinct peak in the atmosphere. The height of this peak descends with decreasing magnitude of absorption. When insufficient number of *k*-intervals are used, the heating profiles attributable to individual intervals are widely separated. Consequently, the total heating exhibits strong oscillation. The oscillation can only be reduced by increasing the number of *k*-intervals. It is found that at least ten *k*-intervals are required to avoid significant oscillation in the heating profile.

Parameterizations for the absorption of solar radiation by ozone follow that of Chou (1992), except that the UV and visible spectral regions are divided into eight bands so that fluxes in the PAR, UV-A, UV-B, and UV-C bands can be separately computed. An effective coefficient for ozone absorption and an effective extinction coefficient for Rayleigh scattering are derived for each band. This spectral separation is important for middle atmospheric studies where photochemical processes are important and for biosphere–atmosphere interaction studies where photosynthesis is important.

Acknowledgments. This work was supported by the Global Atmospheric Modeling and Analysis Program, Office of Mission to Planet Earth, NASA Headquarters. The authors are grateful to Dr. Xun Zhu for his invaluable review of the manuscript.

REFERENCES

Briegleb, B. P., 1992: Delta-Eddington approximation for solar radiation in the NCAR community climate model. *J. Geophys. Res.*, **97,** 7603–7612.

Chou, M.-D., 1990: Parameterization for the absorption of solar radiation by O_2 and CO_2 with application to climate studies. *J. Climate,* **3,** 209–217.

——, 1992: A solar radiation model for use in climate studies. *J. Atmos. Sci.,* **49,** 762–772.

——, and A. Arking, 1981: An efficient method for computing the absorption of solar radiation by water vapor. *J. Atmos. Sci.,* **38,** 798–807.

Kratz, D. P., and R. D. Cess, 1985: Solar absorption by atmospheric water vapor: A comparison of radiation models. *Tellus,* **37B,** 53–63.

Lacis, A. A., and J. E. Hansen, 1974: A parameterization for the absorption of solar radiation in the earth's atmosphere. *J. Atmos. Sci.,* **31,** 118–133.

McClatchey, R. A., R. W. Fenn, J. E. A. Selby, F. E. Volz, and J. S. Garing, 1972: *Optical Properties of the Atmosphere.* 3d ed., Air Force Cambridge Research Laboratories AFCRL-72-0497, 108 pp. [NTIS N7318412]

Ramaswamy, V., and S. M. Freidenreich, 1991: Solar radiative line-by-line determination of water vapor absorption and water cloud extinction in inhomogeneous atmospheres. *J. Geophy. Res.,* **96,** 9133–9157.

Rothman, L. S., R. R. Gamache, A. Barbe, A. Goldman, L. R. Brown, R. A. Toth, H. M. Pickett, R. L. Poynter, J.-M. Flaud, C. Camy-Peyret, A. Barbe, N. Husson, C. P. Rinsland, and M. A. Smith, 1987: The HITRAN data base: 1986 edition. *Appl. Opt.,* **26,** 4058–4097.

World Meteorological Organization, 1985: Atmospheric ozone, global ozone research and monitoring project. Vol. I, Rep. No. 16, 392 pp.